

Interplay between long range hopping and disorder in topological systems

Beatriz Pérez-González,^{*} Miguel Bello,[†] Álvaro Gómez-León, and Gloria Platero
Instituto de Ciencia de Materiales de Madrid (ICMM-CSIC)

(Dated: April 25, 2022)

We extend the standard SSH model to include long range hopping and disorder, and study how the electronic and topological properties are affected. We show that long range hopping can change the symmetry class and the topological invariant, while diagonal and off-diagonal disorder lead to Anderson localization. Interestingly we find that the Lyapunov exponent $\gamma(E)$ can be linked in two ways to the topological properties in the presence of disorder: Either due to the different response of mid-gap states to increasing disorder, or due to an extra contribution to γ due to the presence of edge modes. Finally we discuss its implications in realistic transport measurements.

Introduction: The dimer chain is a canonical model in condensed matter, widely used to study topological properties in systems like polyacetylene, i.e., atomic chains with staggered hopping [1–4]. For the case of just nearest neighbors hopping (NN) and pristine samples, it reduces to the well known SSH model [4]. However, the addition of longer range hopping is important, as it is ubiquitous in real systems and its role can be crucial [5–7].

The effect of disorder in quantum systems has been thoroughly studied since the pioneering works of Anderson [8], but its interplay with topology has been mostly focused on the change of the topological invariants [9–12], while its relation with localization properties has been sometimes overlooked, with a few exceptions [13–15].

In this work we discuss the interplay between these different aspects. More concretely, we show that long range hopping connecting sites within the same sublattice breaks chiral symmetry and changes the topological phase, leading to edge modes without the original topological protection. Furthermore, for large enough hopping, they mix with the bulk bands and the system becomes metallic. In contrast, long range hopping connecting different sublattice sites does not break chiral symmetry and allows to increase the value of the topological invariant and the number of edge modes.

In the presence of disorder we find that Anderson localization happens, as typically expected in 1D. However, some differences between diagonal (DD) and off-diagonal disorder (ODD) can be observed, when just NN hopping is present. This is due to their different effect on the symmetries of the system, which modify the edge states topological protection. Furthermore, the localization properties for mid-gap states (only present in the topological phase) and bulk states is different, and the Lyapunov exponent seems to contain an extra contribution due to edge modes. These makes topology and localization intertwine in an interesting way. When next-nearest-neighbors (NNN) hopping is included we show that the effect of both types of disorder is similar, due to the lack of chiral symmetry. However we find that it is possible to find signatures of topology in transport measurements, even deep within the metallic phase and for weak disorder.

Model: The standard SSH model is described in terms of non-interacting, spinless electrons populating a chain with alternating hoppings between neighboring sites. Long range hopping is added by including processes where the electrons hop to sites farther apart, while disorder is modeled by assuming that at each site the parameters follow some distribution. This leads to the following Hamiltonian:

$$H_R = \sum_{|i-j|\leq R} (J_{i,j} + \epsilon_{i,j})c_i^\dagger c_j + \text{H.c.}, \quad (1)$$

where c_i^\dagger creates a fermion at i th site of the chain and $J_{i,j}$, $i \neq j$, is the (real) hopping amplitude connecting the i th and the j th sites in the pristine chain. R is the maximum range of the hopping and we set the zero of energy at the bare on-site energies, so that $J_{i,i} = 0$.

Diagonal and off-diagonal disorder are introduced through $\epsilon_{i,j}$, for $i = j$ and $i \neq j$, respectively. In the numerical results here presented, we have limited ourselves to the case where $\epsilon_{i,j} \in [-w/2, w/2]$ uniformly distributed, although other distributions could be considered as well [16–18]. For the pristine case, we assume that the hopping amplitudes J_{ij} are functions of the distance between sites $n = |i - j|$. Then, to simplify our notation, we can separate processes connecting sites in the same sublattice $J_{i,i\pm n} \equiv J_n$, with n even, and processes connecting sites in different sublattices $J_{2i-n,2i} \equiv J_n$, and $J_{2i+n,2i} \equiv J'_n$, with n odd.

In absence of disorder, one can diagonalize the Hamiltonian in momentum space: $H_R = \sum_k \Psi_k^\dagger \mathcal{H}_R(k) \Psi_k$, where we have defined $\Psi_k = (a_k, b_k)^T$ and used the Fourier transform $c_{2j-1} = \sum_k e^{ikj} a_k / \sqrt{N}$ and $c_{2j} = \sum_k e^{ikj} b_k / \sqrt{N}$, for $j = 1, \dots, N$ (N is the number of unit cells). The Hamiltonian $\mathcal{H}_R(k)$ is a 2×2 matrix with the following structure: even hoppings contribute to diagonal elements, whereas odd hoppings appear in off-diagonal ones. It can be written in the basis of the

Pauli matrices as $\mathcal{H}_R = d_0(k)\mathbf{1} + \vec{d}(k) \cdot \vec{\sigma}$, with

$$d_0(k) = \sum_p 2J_{2p} \cos(pk), \quad d_z(k) = 0, \quad (2)$$

$$d_x(k) = \sum_p \{J'_{2p-1} \cos[(p-1)k] + J_{2p-1} \cos(pk)\}, \quad (3)$$

$$d_y(k) = \sum_p \{J_{2p-1} \sin(pk) - J'_{2p-1} \sin[(p-1)k]\}, \quad (4)$$

where p ranges from 1 to $\lfloor (R+1)/2 \rfloor$ ($\lfloor \cdot \rfloor$ denotes the floor function). The dispersion relation can be readily obtained as $E_{\pm}(k) = d_0(k) \pm |\vec{d}(k)|$, where “+” and “-” correspond to the conduction and valence band, respectively.

Absence of disorder: The Zak phase characterizes the phase acquired by a particle during adiabatic transport across the Brillouin zone (BZ) [19]. For topological systems and closed loops on the BZ, it is shown to be quantized and linked to a topological invariant \mathcal{W} , namely the winding number of the Bloch vector $\vec{d}(k)$ [20].

The standard SSH model has time-reversal, particle-hole and chiral symmetry, and it supports two distinct topological phases $|\mathcal{W}| \in \{1, 0\}$ featuring either a pair of edge states or none [21]. When longer-range hoppings are added, one can either break particle-hole and chiral symmetry if they connect the same sublattice (even hoppings), or keep the symmetries intact if they connect different sublattices (odd hoppings). Even hoppings change the topological class from BDI to AI, which is topologically trivial in 1D [22], while odd hoppings do not change the topological class and allow for larger values of the topological invariant [23]. The maximum value for the topological invariant is ultimately fixed by the range of the hoppings considered $|\mathcal{W}| \leq (R+1)/2$. Finding a closed expression for the winding number as a function of the system parameters is in general a hard task for couplings beyond NNN [24]. In the supplementary material [25], we show how this can be done for third neighbors and its generalization to an arbitrary number of odd neighbors.

Interestingly, with arbitrary long range hopping the system may still feature edge states, but there is not a one-to-one correspondence between the number of edge states and the topological invariant. This is because the presence of even hoppings introduces a term proportional to the identity matrix, which does not change the bulk eigenstates (leaving the Zak phase unaffected), but it does modify the energy spectrum, making the bands overlap for sufficiently large values of the even hopping amplitudes, changing the system from insulating to metallic (see Fig. 1) [5].

In a finite system, the presence of even hoppings also affects the spatial dependence of the mid-gap states wavefunction, as they do not come in chiral pairs anymore. In general, the localization length of the edge states diverges as they enter the bulk bands when increasing the

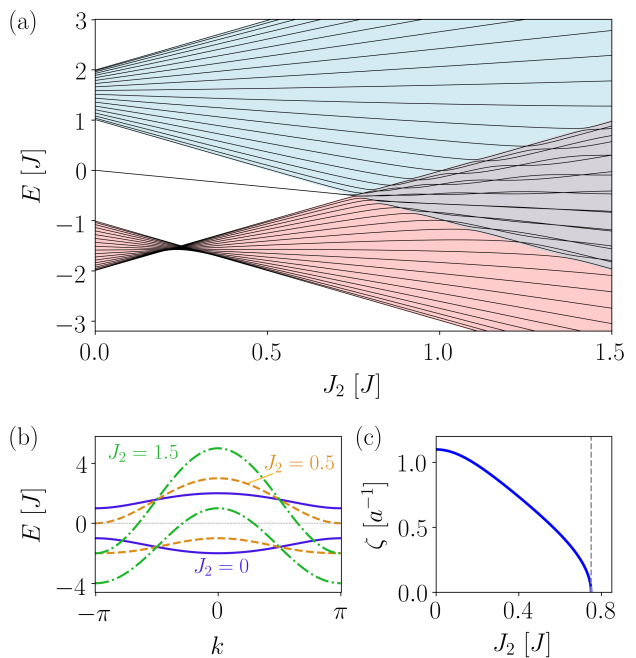


FIG. 1. (a) Spectrum vs J_2 for a finite system. (b) Spectrum vs quasimomentum k for different values of J_2 . (c) Inverse of localization length vs J_2 for the edge states. All plots consider a pristine chain with first- and second-neighbour hoppings, being $\delta = -0.5$. Notice the transition to a metallic phase for $J_2 = 0.75J$, with the edge modes entering the bulk bands.

strength of the even hopping amplitudes. This can be seen already for NNN hoppings. Using perturbation theory, one can show that the energy of the edge states varies as $E_{\text{edge}} \simeq -2J_2 J'_1 / J_1$ [25]. Then, looking for solutions of the dispersion relation with complex quasi-momentum $k = \pi \pm i\zeta$ we arrive at the following expression for the inverse of the localization length:

$$\zeta = \frac{1}{\lambda_{\text{loc}}} = \text{acosh} \left[\frac{J'_1}{J_1} - \frac{J_1 J'_1}{4J_2^2} + \frac{1}{4J_2^2} \sqrt{4J_2^2 (J_1^2 - J_1'^2) + J_1^2 J_1'^2} \right], \quad (5)$$

which is plotted in Fig.1 (c).

In the following, we focus on the effect of disorder, as well as on the transport properties with NNN present. For convenience, we re-parameterize $J_1 = J(1 - \delta)$ and $J'_1 = J(1 + \delta)$ in terms of the dimerization factor δ , and the average NN hopping J . Importantly, the topologically non-trivial phase ($|\mathcal{W}| = 1$) occurs for $\delta < 0$, while the trivial phase ($|\mathcal{W}| = 0$) occurs for $\delta > 0$.

Disorder: We have so far discussed how the topological properties are affected by adding long range hopping, which can drastically change due to the breaking of certain key symmetries. Another way of modifying these symmetries or to investigate changes in the topological properties is by including disorder.

Typically, DD acts within the same sublattice and therefore breaks chiral symmetry. This modifies the topological phase, leads to a splitting of the zero-energy modes and produces localization. On the other hand, ODD maintains the chiral symmetry (in the standard Anderson model this is well known to produce an anomalous density of states and localization in the vicinity of $E \simeq 0$ [17, 18, 26–28]) and makes the topological phase well defined for weak disorder. In this case the edge states remain gapless, but the bulk electrons also localize.

To first gain some intuition about the localization properties in the SSH model, we have calculated a moment expansion of the Lyapunov exponent (LE), i.e., the inverse of the localization length, with NN hopping only [29]:

$$\gamma_D(E) \simeq \log |A| - \frac{E^2 \sigma^2}{(E^2 - 4J^2)(E^2 - 4J^2 \delta^2)} \quad (6)$$

$$\gamma_O(E) \simeq \log |A| - \frac{h(E) \sigma^2}{2(A^2 - 1)^2 J_1^2 J_1'^2} \quad (7)$$

where $A(E) = \left[f(E) \pm \sqrt{f(E)^2 - 4J_1^2 J_1'^2} \right] / 2J_1 J_1'$, $f(E) = E^2 - J_1^2 - J_1'^2$ and $h(E) = (A^4 - 8A^2 - 1)J_1^2 - 4A(A^2 + 3)J_1 J_1' + (A^4 - 8A^2 - 1)J_1'^2$ (Details of the calculation in the Supplemental Material [25]). Fig.2(b) shows a comparison between the two analytic formulas, which show similar behavior with the exception that ODD produces stronger localization. This is expected because values of the hopping close to zero correspond to full localization.

One can check that Eqs. (6) and (7) recover the expressions for the Anderson model obtained by the same method: $\gamma(E) \propto -\sigma^2/(E^2 - 4J^2)$ (valid for both DD and ODD, being the prefactors the only difference between the two cases), in the limit $\delta \rightarrow 0$. Importantly, as Eqs.(6) and (7) do not depend on the sign of the dimerization factor δ , the trivial and topological phases cannot be distinguished by their localization properties for weak disorder, at least to second order in the perturbative expansion. This is also expected because topological properties are not captured by local quantities.

Interestingly, due to the poles structure in Eqs. (6) and (7), one has a crossover region within the gap where localization is anomalous, changing sign for the states in the gap, which become less localized for increasing disorder. This is well known in non-topological systems, but topological systems provide an extra twist: they display mid-gap states (only present in the topological phase) that will delocalize as disorder increases, while the bulk states will localize more. This is important for measurements that depend only on these mid-gap states, such as edge modes transport.

As a check we have calculated numerically the Green's function $G = (E - H)^{-1}$, and by fitting the disorder-averaged elements $-\log(\langle G_{1,L}^2 \rangle)$, ($L = 1, \dots, 2N$), we

have obtained $\gamma(E)$ from its slope. Fig.2(a) shows the LE vs E for different values of diagonal disorder and a comparison with the analytical expression for weak disorder. There one can see that for weak disorder the agreement is excellent and captures the previously discussed delocalization of midgap states. For large disorder these phenomenon disappears and all states become more localized for increasing w .

An interesting property missing in the perturbative calculation is shown in Fig.2(b). It shows that the difference between the $\gamma(E = 0)$ in the trivial and in the topological phase, when ODD is added, is non-vanishing as a function of disorder strength (with variance always smaller than this difference). We have checked that this difference is stable for different system lengths ($N = 50, 100, 150$ and 200), which means that it should remain in the limit $N \rightarrow \infty$. Furthermore, this difference scales $\propto \sigma^2$, which would indicate that it does not correspond to higher orders in the perturbative expansion. Therefore, the fact that it remains in the thermodynamical limit and that it does not appear in the formula for the bulk Lyapunov exponent to second order, would indicate that this contribution is consequence of the presence of the edge modes.

When one includes NNN hopping, the electronic properties can be severely affected due to the changes in the energy bands, and specially due to the transition to a metallic phase with electron and hole pockets for large J_2 . Fig.3 shows the value of $\gamma(E)$ for different values of J_2 and disorder. For small J_2 the chiral symmetry is weakly broken and the system still displays a gap. As J_2 increases, the bands and the Lyapunov exponent become increasingly asymmetrical. It is interesting to see how diagonal and off-diagonal disorder act in a similar way when NNN are present (compare purple and orange lines in Fig.3). This is because chiral symmetry is already broken by J_2 , and then off-diagonal disorder also introduces fluctuations within the same sublattice [30]. For large J_2 the system becomes metallic and although the Lyapunov exponent behaves similarly for DD and ODD, we will see next that transport in the trivial and in the topological phase, can be quite different for small disorder.

Single-particle transport:

Coupling the ends of the SSH chain to voltage-biased leads allows for particle transport. We use second-order perturbation theory to integrate out the leads, and obtain a master equation for the reduced density matrix of the chain [31, 32]. In the infinite bias regime transport is unidirectional and the master equation assumes the following Lindblad form:

$$\dot{\rho} = \mathcal{L}\rho \equiv -i[H_R, \rho] + \Gamma_L \mathcal{D}(c_1^\dagger)\rho + \Gamma_R \mathcal{D}(c_{2N})\rho, \quad (8)$$

where $\mathcal{D}(A)\rho \equiv A\rho A^\dagger - \{A^\dagger A, \rho\}/2$. The last two terms in the r.h.s of equation (8) correspond to incoherent tun-

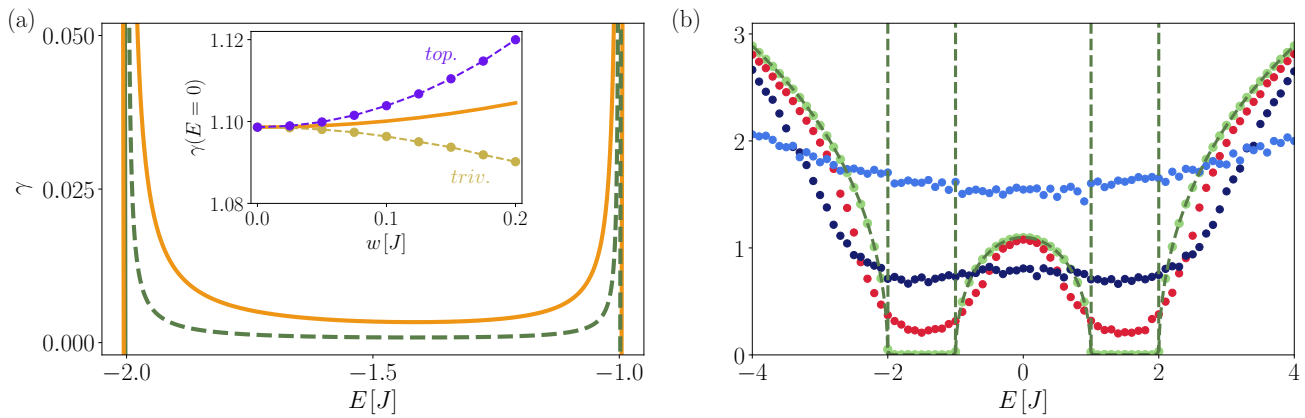


FIG. 2. (a) Plot of Eq.(7) (orange) and Eq.(6) (dark green) for the states in the band with $J = 1$, $\delta = -0.5$ and $w/J = 0.1$. Inset: difference between the $\gamma(E = 0)$ in the trivial (yellow) and topological (purple) phase in the presence of ODD in the SSH chain as a function of w , compared to the analytic formula in Eq.(7). (b) Lyapunov exponent vs energy for different DD strengths w in the SSH model. The dashed line (dark green) corresponds to the analytical approximation (Eq.6) and the dots to the exact numerical calculation using Green's functions. Parameters: $J = 1$, $\delta = -0.5$ and $w/J = 0.1$, (light green) 2 (red), 4 (dark blue) and 10 (light blue).

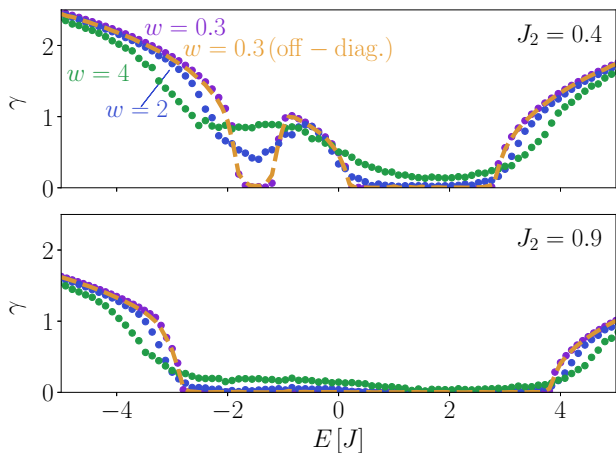


FIG. 3. Lyapunov exponent vs E for a chain with fixed NN hoppings and different values of the NNN hoppings. The dotted lines correspond to diagonal disorder, while the dashed line corresponds to off-diagonal disorder. Parameters: $J = 1$, $\delta = -0.5$, $w/J = 0.3$ (purple for diagonal and orange for off-diagonal), 2 (blue), 4 (green), $J_2/J = 0.4$ (upper plot), 0.9 (lower plot).

neling of particles from the left lead into the first site of the chain at rate Γ_L , and tunneling out from the last site of the chain to the right lead at rate Γ_R .

We have analyzed the transport considering there is at most one particle in the system. This is the case if the interaction between particles inside the chain is strong enough such that higher chain occupancies are forbidden. The current in the stationary regime can be computed as $I = \text{tr}(\mathcal{J}\rho_0)$, where ρ_0 is the stationary solution of the master equation (8) and $\mathcal{J}\rho = \Gamma_L c_1^\dagger \rho c_1$ (or alternatively $\mathcal{J}\rho = \Gamma_R c_{2N}^\dagger \rho c_{2N}$) is the current superoperator.

In Fig. 4, we show the current in a pristine dimer chain with hoppings up to 2nd neighbors as a function of the different hopping amplitudes. The results show a striking difference between the current in the topological and the trivial regimes for all values of J_2 . In the regime where the chain is insulating, we find the *topological edge-state blockade* already studied in [32, 33]. As J_2 increases, the topological edge-state blockade remains up to the transition to the metallic phase; however, the trivial region ($\delta > 0$) displays a line of vanishing current $J_2 \simeq -\delta J/2 + J/2$, that corresponds to a configuration where the lower energy band is almost flat. For large enough J_2 the system enters the metallic phase, showing a pattern of diamonds in the topological phase. In the trivial phase there is also an interesting pattern in the metallic region. This patterns correspond to dips in the current produced by exact crossings of energy levels with opposite parity (see Fig. 1). Whenever two states with opposite parity become degenerate, a superposition of both of them with zero occupation at the ending site of the chain becomes a steady state of the system. A particle in this superposition prevents any new particle from tunneling into the system, and it cannot escape to the drain, thus blocking the current. Remarkably, most of these degeneracies occur for the same values $|\delta|$ and J_2/J in the topological and the trivial regime. Nonetheless, most of the dips in the trivial regime cannot be appreciated in Fig. 4 since they are very sharp. The reason why resides in the way these states in the bands overlap split in the neighborhood of the crossings and also in the weight that they have on the ending sites of the chain [25], which determines their importance to the transport. This latter fact becomes evident after plotting the local density of states at the edge sites of the chain, which can be computed efficiently with a recursive formula for the

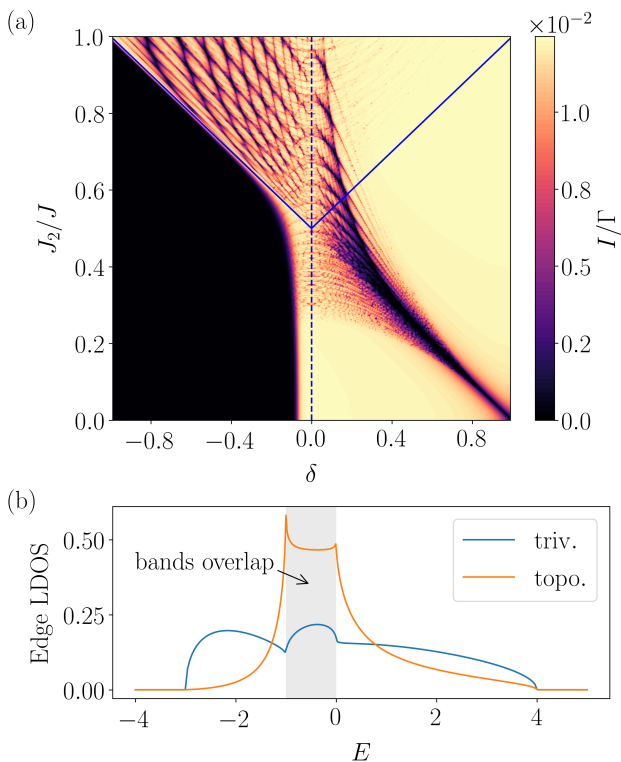


FIG. 4. (a) Current with $\Gamma_L = \Gamma_R = 0.1J$, for a chain with $N = 40$ dimers. The dashed vertical line marks the topological phase transition, while the upper triangle delimited by continuous lines marks the region where the system is metallic. (b) Local density of states at the ending sites for a semi-infinite system for $J_2 = J$ and $\delta = -0.5$ (topological case) or $\delta = 0.5$ (trivial case).

lattice Green function [34].

We have, as well, computed the Fano factor, which is a measure of the shot noise in the transport process. Previous studies showed that for the standard SSH model the Fano factor is approximately equal to 1 in the topological regime [32], meaning that the transport is purely Poissonian. We have found that for finite J_2 it generally is larger than 1, and it presents clear differences between the topological and the trivial phases. In the metallic region, it has peaks or dips at the exact crossings discussed above. The shape of these features is directly related to the LDOS at the edges of the chain and therefore reflects the topology of the system [25].

The effect of disorder on the current when hoppings up to NNN are included is similar for both the DD and ODD cases [25]. For small disorder there is some difference between the trivial and the topological phase that fades out as disorder increases. Near the exact crossings, the current shows a non-monotonic behavior in the topological phase: it increases for small disorder and decreases for large disorder.

Conclusions: In this work, we have studied a generalized model for a dimer chain including long-range hop-

ping and disorder, which naturally occur in many physical systems. We have shown that the effect of hopping connecting sites within the same sublattice (even hopping), and those connecting sites of different sublattices (odd hopping) is very different. The reason is that the former break particle-hole and chiral symmetry, changing the topological class, while the later maintains chiral symmetry and allows to increase the value of the winding number. When both types of hopping are considered, space inversion symmetry is present, forcing the topological invariant to still have quantized values. This means that edge states are protected only by this symmetry, but now the bulk-edge correspondence does not hold anymore, specially when the NNN hopping is large, which results in a metallic phase and the merging of the edge states into the bulk bands.

The role of disorder has been studied by means of the Lyapunov exponent. We have shown that for NN hopping only, DD and ODD localize the bulk electrons, but their effect on midgap states is different, with a crossover from reduced to increased localization as a function of diagonal disorder strength. In addition, our numerical calculations find an extra contribution to $\gamma(E)$, as a function of off-diagonal disorder strength, that leads to a difference between the trivial and the topological phase. This contribution seems to be linked to the presence of edge modes in a topological system with boundaries. When NNN are added, chiral symmetry is broken and fluctuations in J_2 act similarly to DD. Nevertheless we have shown that transport measurements for weak disorder, can still distinguish between phases with different winding number. Furthermore, the current in the metallic phase shows interesting features that also allow to differentiate between the topological and trivial phases.

Our findings could be observed experimentally with arrays of quantum dots [35], in which the large Coulomb repulsion needed to keep at most one electron in the system could be engineered by capacitively coupling all dots together. Also, our results are relevant to the transport of excitations in analogue systems, which could be implemented in platforms such as trapped ions [36] or cold atoms [37, 38].

ACKNOWLEDGEMENTS

This work was supported by the Spanish Ministry of Economy and Competitiveness through Grant No.MAT2014-58241-P and Grant MAT2017-86717-P. M. Bello acknowledges the FPI program BES-2015-071573, Á. Gómez-León acknowledges the Juan de la Cierva program and Beatriz Pérez-González acknowledges the FPU program FPU17/05297.

* bperez03@ucm.es

† miguel.bello@icmm.csic.es

- [1] R. Peierls, *Quantum theory of solids* (Oxford University Press, 1955).
- [2] R. Jackiw and C. Rebbi, Phys. Rev. D **13**, 3398 (1976).
- [3] W. P. Su, J. R. Schrieffer, and A. J. Heeger, Phys. Rev. Lett. **42**, 1698 (1979).
- [4] W. P. Su, J. R. Schrieffer, and A. J. Heeger, Phys. Rev. B **22**, 2099 (1980).
- [5] M. Di Liberto, D. Malpetti, G. I. Japaridze, and C. Morais Smith, Phys. Rev. A **90**, 023634 (2014).
- [6] O. Viyuela, L. Fu, and M. A. Martin-Delgado, Phys. Rev. Lett. **120**, 017001 (2018).
- [7] W. DeGottardi, M. Thakurathi, S. Vishveshwara, and D. Sen, Phys. Rev. B **88**, 165111 (2013).
- [8] P. W. Anderson, Phys. Rev. **109**, 1492 (1958).
- [9] C. W. Groth, M. Wimmer, A. R. Akhmerov, J. Tworzydło, and C. W. J. Beenakker, Phys. Rev. Lett. **103**, 196805 (2009).
- [10] J. Li, R.-L. Chu, J. K. Jain, and S.-Q. Shen, Phys. Rev. Lett. **102**, 136806 (2009).
- [11] G. Schubert, H. Fehske, L. Fritz, and M. Vojta, Phys. Rev. B **85**, 201105 (2012).
- [12] E. V. Castro, M. P. López-Sancho, and M. A. H. Vozmediano, Phys. Rev. B **92**, 085410 (2015).
- [13] T. Rakovszky and J. K. Asboth, Phys. Rev. A **92**, 052311 (2015).
- [14] A. Altland, D. Bagrets, and A. Kamenev, Phys. Rev. B **91**, 085429 (2015).
- [15] T. Liu and H. Guo, Physics Letters A (2018), <https://doi.org/10.1016/j.physleta.2018.09.023>.
- [16] T. Odagaki, Solid State Communications **33**, 861 (1980).
- [17] A. D. Stone and J. D. Joannopoulos, Phys. Rev. B **24**, 3592 (1981).
- [18] C. M. Soukoulis and E. N. Economou, Phys. Rev. B **24**, 5698 (1981).
- [19] J. Zak, Phys. Rev. Lett. **62**, 2747 (1989).
- [20] P. Delplace, D. Ullmo, and G. Montambaux, Phys. Rev. B **84**, 195452 (2011).
- [21] J. Asbóth, L. Oroszlány, and A. Pályi, *A Short Course on Topological Insulators: Band Structure and Edge States in One and Two Dimensions*, Lecture Notes in Physics (Springer International Publishing, 2016).
- [22] S. Ryu, A. P. Schnyder, A. Furusaki, and A. W. W. Ludwig, New Journal of Physics **12**, 065010 (2010).
- [23] B.-H. Chen and D.-W. Chiou, .
- [24] L. Li, Z. Xu, and S. Chen, Phys. Rev. B **89**, 085111 (2014).
- [25] See Supplementary Material.
- [26] L. Fleishman and D. C. Licciardello, Journal of Physics C: Solid State Physics **10**, L125 (1977).
- [27] H. Cheraghchi, S. M. Fazeli, and K. Esfarjani, Phys. Rev. B **72**, 174207 (2005).
- [28] C. Zhou and R. N. Bhatt, Phys. Rev. B **68**, 045101 (2003).
- [29] R. P. Budoyo, *Conductance in Mesoscopic Rings*, Ph.D. thesis, Wesleyan University, Connecticut (2008).
- [30] M. Inui, S. A. Trugman, and E. Abrahams, Phys. Rev. B **49**, 3190 (1994).
- [31] H. Breuer and F. Petruccione, *The Theory of Open Quantum Systems* (OUP Oxford, Great Clarendon Street, Oxford OX2 6DP, 2007).
- [32] M. Benito, M. Niklas, G. Platero, and S. Kohler, Phys. Rev. B **93**, 115432 (2016).
- [33] L. Ruocco and A. Gómez-León, Phys. Rev. B **95**, 064302 (2017).
- [34] M. Möller, A. Mukherjee, C. P. J. Adolphs, D. J. J. Marchand, and M. Berciu, Journal of Physics A: Mathematical and Theoretical **45**, 115206 (2012).
- [35] D. M. Zajac, T. M. Hazard, X. Mi, E. Nielsen, and J. R. Petta, Phys. Rev. Applied **6**, 054013 (2016).
- [36] P. Nevado, S. Fernández-Lorenzo, and D. Porras, Phys. Rev. Lett. **119**, 210401 (2017).
- [37] E. J. Meier, A. A. Fangzhao, A. Dauphin, M. Maffei, P. Massignan, T. L. Hughes, and G. Bryce, arXiv:1802.02109.
- [38] L. Sanchez-Palencia and M. Lewenstein, Nature Physics **6**, 87–95 (2010).